

# Implications of the CMS search for $W_R$ on Grand Unification

Triparno Bandyopadhyay<sup>1\*</sup>, Biswajoy Brahmachari<sup>2†</sup>, and Amitava Raychaudhuri<sup>1‡</sup>

(1) Department of Physics, University of Calcutta,  
92 Acharya Prafulla Chandra Road, Kolkata 700009, India

(2) Department of Physics, Vidyasagar Evening College,  
39 Sankar Ghosh Lane, Kolkata 700006, India



The CMS experiment at the Large Hadron Collider has reported a  $2.8\sigma$  excess in the  $(2e)(2jets)$  channel around 2.1 TeV. Interpretation of this data in terms of the production of a right-handed weak gauge boson,  $W_R$ , of the left-right symmetric model and in an  $SO(10)$  grand unified theory is reconsidered. The left-right symmetric model can be consistent with this excess if (a) the heavy right-handed neutrino has a mass near  $W_R$ , or (b) if  $g_L \neq g_R$ , or (c) the right-handed CKM matrix is nontrivial. Combinations of the above possibilities are also viable. A  $W_R$  with a mass in the TeV region if embedded in  $SO(10)$  is not compatible with  $g_L = g_R$ . Rather, it implies  $0.64 \leq g_R/g_L \leq 0.78$ . Further, a unique symmetry-breaking route – the order being left-right discrete symmetry breaking first followed by  $SU(4)_C$  and finally  $SU(2)_R$  – to the standard model is picked out. The  $L \leftrightarrow R$  discrete symmetry has to be broken at around  $10^{17}$  GeV. The grand unification scale is pushed to  $10^{18}$  GeV making the detection of proton decay in ongoing searches rather unlikely. The  $SU(4)_C$  breaking scale can be at its allowed lower limit of  $10^6$  GeV so that  $n - \bar{n}$  oscillation or flavour changing processes such as  $K_L \rightarrow \mu e$  and  $B_{d,s} \rightarrow \mu e$  may be detectable. The Higgs scalar multiplets responsible for symmetry breaking at various stages are uniquely identified so long as one adheres to a minimalist principle. We also remark, *en passant*, about a partially unified Pati-Salam model.

Key Words: Left-right symmetry, Right-handed gauge boson, Grand Unification, LHC

arXiv:1409.4052 [hep-ph]

$$\mathcal{L}^{CC} = \frac{g_L}{\sqrt{2}} \bar{U}_L \gamma^\mu V_L D_L W_{L\mu}^+ + \frac{g_R}{\sqrt{2}} \bar{U}_R \gamma^\mu V_R D_R W_{R\mu}^+ + \text{h.c.},$$

\*email: gondogolegogol@gmail.com

†email: biswa.brahmac@gmail.com

‡email: palitprof@gmail.com

and force carriers of the SM now detected and the source of spontaneous symmetry breaking identified there is a well-deserved sense of satisfaction. Nonetheless, there is a widely shared expectation that there is new physics which may be around the corner and within striking range of the LHC. The shortcomings of the standard model are well-known. There is no candidate for dark matter in the SM. The neutrino is massless in the model but experiments indicate otherwise. At the same time the utter smallness of this mass is itself a mystery. Neither is there any explanation of the matter-antimatter asymmetry seen in the Universe. Besides, the lightness of the Higgs boson remains an enigma if there is no physics between the electroweak and Planck scales.

Of the several alternatives of beyond the standard model extensions, the one on which we focus in this work is the left-right symmetric (LRS) model [1, 2] and its embedding within a grand unified theory (GUT). Here parity is a symmetry of the theory which is spontaneously broken resulting in the observed left-handed weak interactions. The left-right symmetric model is based on the gauge group  $SU(2)_L \times SU(2)_R \times U(1)_{B-L}$  and has a natural embedding in the  $SU(4)_C \times SU(2)_L \times SU(2)_R$  Pati-Salam model [3] which unifies quarks and leptons in an  $SU(4)_C$  symmetry. The Pati-Salam symmetry is a subgroup of  $SO(10)$  [4, 5]. These extensions of the standard model provide avenues for the amelioration of several of its shortcomings alluded to earlier.

The tell-tale signature of the LRS model would be observation of the  $W_R$ . At the LHC the CMS collaboration has searched for the on-shell production of a right-handed charged gauge boson [6] using the process<sup>1</sup>:

$$pp \rightarrow W_R \rightarrow 2j + ll \quad . \quad (1)$$

arXiv:1306.2342v2 [hep-ph]

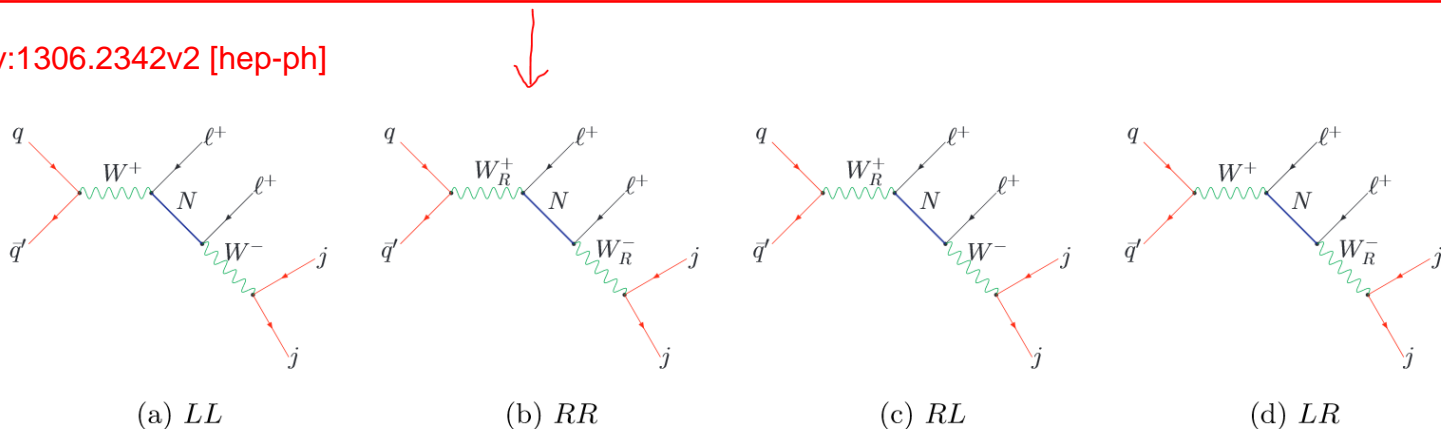


FIG. 1. The Feynman diagrams contributing to the ‘smoking gun’ collider signal of seesaw in the minimal L-R model.

example, in [11] - [14].

In a left-right symmetric model emerging from a grand unified theory, such as  $SO(10)$ , one has a discrete symmetry  $SU(2)_L \leftrightarrow SU(2)_R$  – referred to as D-parity [15] – which sets  $g_L = g_R$ . Both D-parity and  $SU(2)_R$  are broken during the descent of the GUT to the standard model, the first making the coupling constants unequal and the second resulting in a massive  $W_R$ . The possibility that the energy scale of breaking of D-parity is different from that of  $SU(2)_R$  breaking is admissible and well-examined. The difference between these scales and the particle content of the theory controls the extent to which  $g_L \neq g_R$ .

<sup>1</sup>Earlier searches at the LHC for the  $W_R$  can be found in [7, 8].

<sup>2</sup>The existence of three right-handed neutrinos –  $N_e, N_\mu$  and  $N_\tau$  – is acknowledged.

In this work we consider the different options of  $SO(10)$  symmetry breaking. It is shown that a light  $W_R$  goes hand-in-hand with the breaking of D-parity at a high scale, immediately excluding the possibility of  $g_L = g_R$ . Breaking of D-parity above the scale of inflation, in fact, is usually considered a good feature for getting rid of unwanted topological defects such as domain walls [16, 17]. The other symmetries that are broken in the passage to the standard model are the  $SU(4)_C$  and  $SU(2)_R$  of the Pati-Salam (PS) model. The stepwise breaking of these symmetries and the order of their energy scales have many variants. There are also a variety of options for the scalar multiplets which are used to trigger the spontaneous symmetry breaking at the different stages. We take a minimalist position of (a) not including any scalar fields beyond the ones that are essential for symmetry breaking, and also (b) impose the Extended Survival Hypothesis (ESH) corresponding to minimal fine-tuning to keep no light extra scalars. With these twin requirements we find that only a single symmetry-breaking route – the one in which the order of symmetry breaking is first D-parity, then  $SU(4)_C$ , and finally  $SU(2)_R$  – can accommodate a light  $M_{W_R}$ . We find that one must have  $0.64 \leq g_R/g_L \leq 0.78$ .

The paper is divided as follows. In the following section we give details of the CMS result [6] which are relevant for our discussion within the context of the left-right symmetric model. In the next section we elaborate on the GUT symmetry-breaking chains, the extended survival hypothesis for light scalars, and coupling constant evolution relations. Next we briefly note the implications of coupling constant unification within the Pati-Salam and  $SO(10)$  models. The results which emerge for the different routes of descent of  $SO(10)$  to the SM are presented in the next two sections. We end with our conclusions.

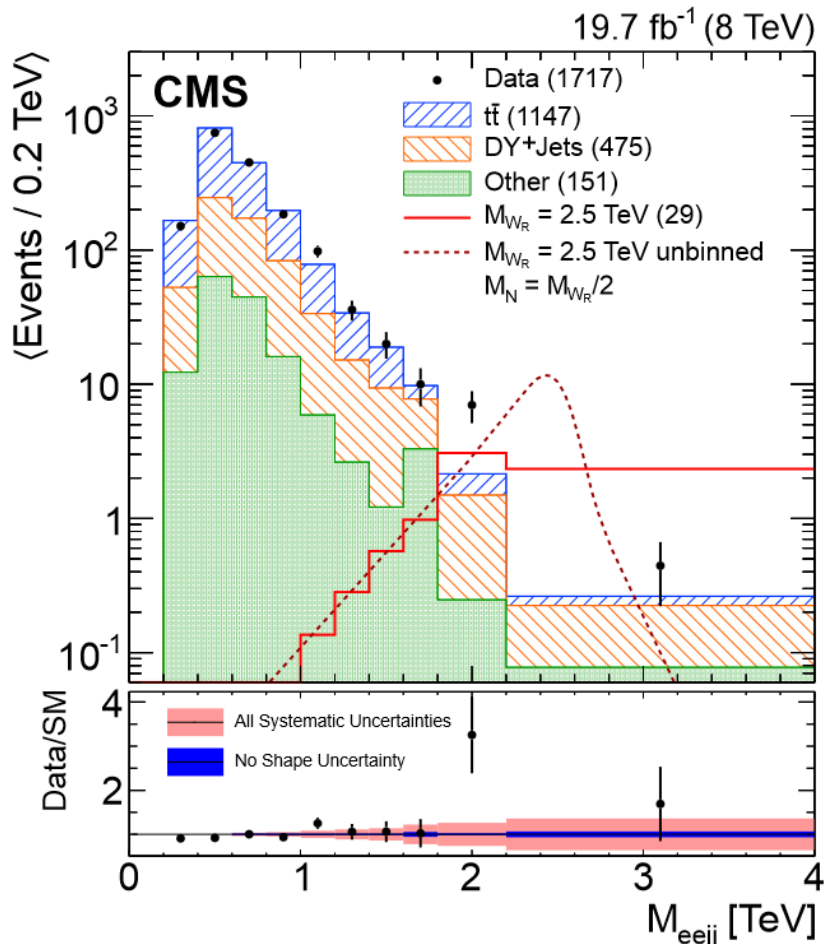
## II CMS $W_R$ search result and the Left-Right Symmetric model

The results of the CMS collaboration for the LHC run at  $\sqrt{s} = 8$  TeV with an integrated luminosity of  $19.7 \text{ fb}^{-1}$  are shown in Fig. 1. The production of a  $W_R$  which then decays to a charged lepton and a quark which are on-shell. The  $N_l$  undergoes a cascade decay into quarks which manifest as hadronic jets ( $2j$ ) or leptons ( $2l$ ) data within the framework of an LRS model in the  $M_{W_R} - M_{N_l}$  plane<sup>3</sup>. Interpreting the excess in the supplementary material of [6], the CMS collaboration finds that  $\sigma(pp \rightarrow W_R) \times BR(W_R \rightarrow lljj) \equiv \sigma BR$  as shown in Fig. 1. In the electron channel, irrespective of the expected exclusion limit ( $\sigma BR_E$ ) for  $M_{W_R} \leq 2.1$  TeV. Though not large enough for a firm discovery, and if this is correct, one can expect confirmation of the  $W_R$  signal. The CMS collaboration notes that this excess is consistent with  $W_R$  production and no leptonic mixing. As we stress later, the CMS results agree with the left-right symmetric model.

### II.1 A $W_R$ signal?

Fig. 1 shows the Feynman diagram for  $W_R$  production and decay [18]. Note that the production of the  $W_R$

<sup>3</sup>An alternate explanation of the excess in the data is given in [19].



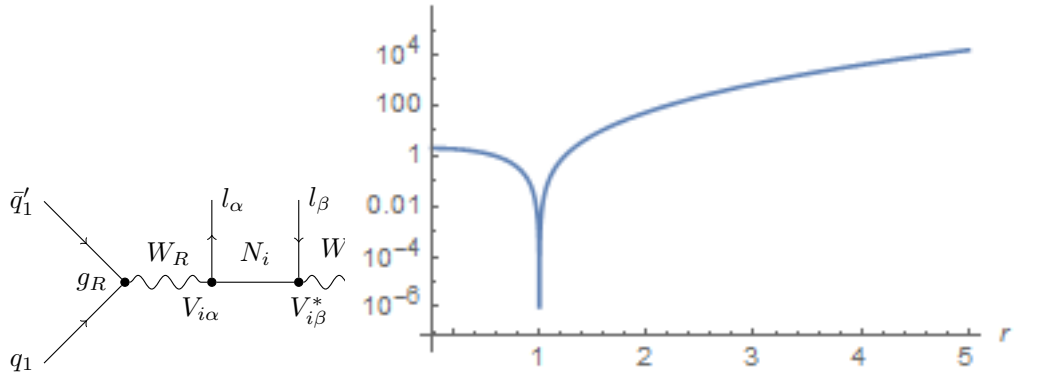


Figure 1: *Feynman diagram of the process under discussion with the right-handed CKM-like mixing matrix taken in a general, non-diagonal, form*

boson of the same mass by a factor  $\eta^2$ , where  $\eta = (g_R/g_L)$ . The contribution from this diagram is determined by  $S^2$  where  $S \equiv \eta|V_{N_e e}|^2$ . Neglecting the masses of the final state quarks and the charged lepton, the branching ratio of the three-body decay of  $N_e$ , which we have calculated, is proportional to  $(1 - r^2)^2(2 + r^2)$ , where, as noted earlier,  $r = M_{N_e}/M_{W_R}$ . **A clinching evidence of this process would then be a peak in the  $(2e)(2j)$  invariant mass at  $M_{W_R}$  – for which there is already a hint – along with another around  $M_{N_e}$  in the invariant mass of one of the two  $e(2j)$  combinations in every event. The latter is awaited.**

It has to be borne in mind that **the excess seen in the  $(2e)(2j)$  mode is not matched in the  $(2\mu)(2j)$  data.** This would have to be interpreted as an indication that the right-handed neutrino associated with the muon,  $N_\mu$ , is significantly heavier than  $N_e$  and so its production in  $W_R$ -decay suffers a large kinematic suppression. Further, the coupling of  $N_e$  to  $\mu$  has to be small, which implies that  $|V_{N_e \mu}| \ll 1$ .

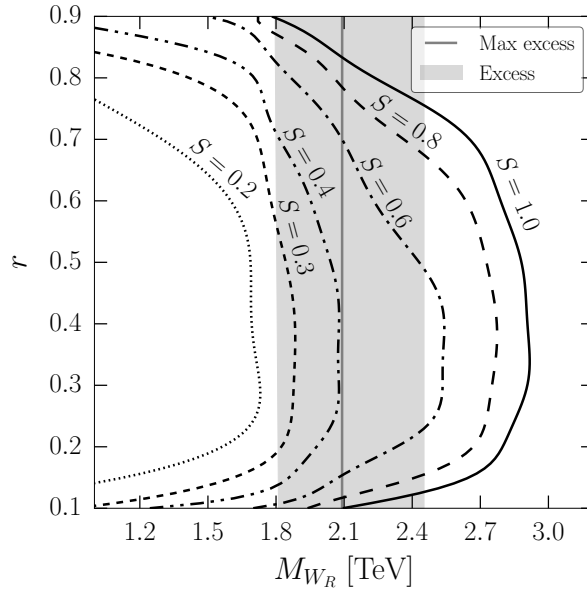


Figure 2: *The shaded region demarcates the range of  $M_{W_R}$  for which the CMS data exceed twice the SM expectation. The maximum excess is on the vertical straight line. The curves parametrised by  $S$  denote the  $(r, M_{W_R})$  contours for which the prediction of the LRS model is compatible with the observation.*

In Fig. 2 we place the excess observed by CMS in this channel – the shaded region in the  $M_{W_R} - r$  plane – in comparison with the LRS model predictions. This excess is maximum along the vertical line. The expectations from the Left-Right Symmetric model ( $\sigma BR_T$ ) depend on  $S^2 = \eta^2|V_{N_e}|^4$  and

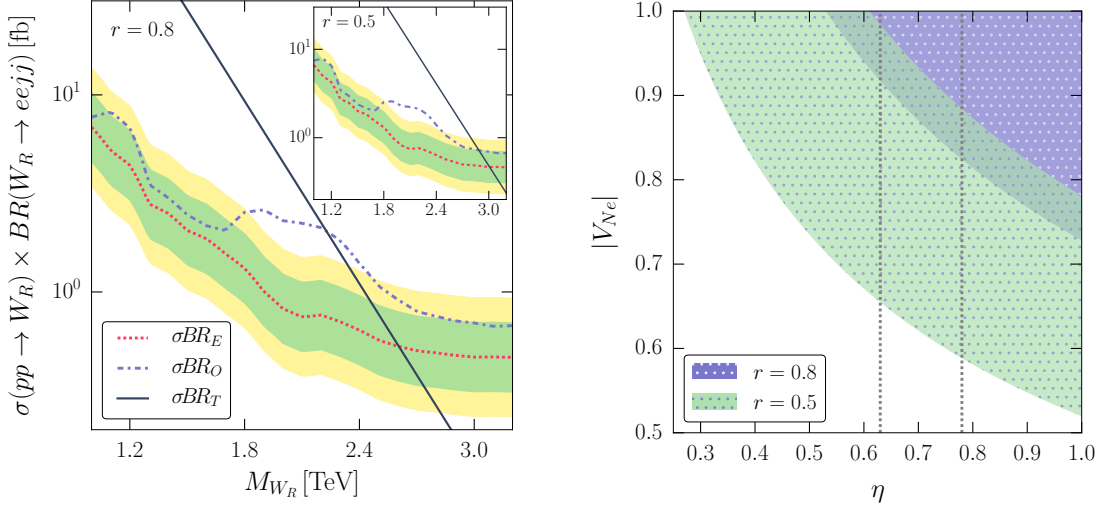


Figure 3: *Left:* The CMS data compared with the LRS model predictions for  $r = 0.8$  keeping  $g_R/g_L = 1$  and  $V_{N_e} = 1$ . *Inset:*  $r = 0.5$ . *Right:*  $\eta$  and  $V_{N_e}$  that fit the excess in the CMS data for  $r = 0.5$  and  $r = 0.8$ . Only the region between the two vertical lines is permitted in  $SO(10)$  GUTs.

$r = M_{N_e}/M_{W_R}$ . The dashed curves in the figure, identified by the values of  $S$ , trace the points in the  $(r - M_{W_R})$  plane for which the LRS expectations equal  $\sigma BR_O$ . To put the plot in context note that CMS has stressed [6] that with  $\eta = 1$  and  $V_{N_e} = 1$  – i.e.,  $S = 1$  – the LRS model signal for  $r = 0.5$  is inconsistent with the excess. This is borne out from Fig. 2 which indicates that for the  $S = 1$  contour, the  $M_{W_R}$  corresponding to  $r = 0.5$  lies outside the excess region. Consistency of the excess in the data with the LRS model can be accomplished in three ways. Firstly, if  $r = M_{N_e}/M_{W_R}$  is larger than 0.5 the LRS model signal will be reduced. Indeed, with  $r > 0.75$  the LRS model is consistent with the excess even with  $S = 1$ . Alternatively, if  $\eta$  or  $V_{N_e}$  is less than unity, then too the signal will be less, the suppression being determined by  $S^2$ . In Fig. 2 it can be seen that for  $r = 0.5$  the excess is consistent with the model for  $0.3 \lesssim S \lesssim 0.6$ . The upper limit has been pointed out in [9] and [10]. What we essentially find is that there are large sets of values of  $r$  and  $S$  for which the LRS expectation is consistent with the excess.

Fig. 2 contains information in a somewhat condensed form. In the spirit of the path chosen by the CMS collaboration, we use the exclusion data and plot in the left panel of Fig. 3  $\sigma BR_E$  (red dotted curve) and  $\sigma BR_O$  (blue dashed curve) as functions of  $M_{W_R}$  for the fixed value of  $r = 0.8$ . The prediction of the LRS model with  $\eta = g_R/g_L = 1$  and  $V_{N_e} = 1$  is the black solid straight line. Also, shown are the bands which correspond to an enhancement of the expected cross section by 50% (green) and 100% (yellow). In the inset the same results are presented but for  $r = 0.5$ . Notice that for  $r = 0.8$  the LRS model expectation passes right through the maximum of the excess while for  $r = 0.5$  it entirely misses the excess region.

The right panel of Fig. 3 utilises a complementary way of displaying the region in the LRS model parameter space consistent with the result. Here the area in the  $\eta - V_{N_e}$  plane that fits the CMS excess region is shown shaded for two values of  $r = 0.8$  (dark, violet) and 0.5 (light, green). It is worth stressing that, as in the left panel, for  $r = 0.8$  the model is consistent with the data even for  $\eta = 1$  and  $V_{N_e} = 1$ . For  $r = 0.5$  a suppression through the factor  $S = \eta|V_{N_e}|^2$  is required to bring the model in harmony with the data. If the  $W_R$  with a mass  $\mathcal{O}(\text{TeV})$  arises from the  $SO(10)$  GUT model we discuss

below then  $\eta$  must lie within the two vertical lines.

### III $SO(10)$ Grand Unification

$SO(10)$  is an attractive candidate for a unified theory [4, 5] as it is the simplest Lie group which includes all the SM fermions and a right-handed neutrino of one generation in a single irreducible representation. We do not include any exotic fermions in the model and deal with three generations.

There are a vast number of models characterised by different intermediate symmetries which have  $SO(10)$  as the unifying group. In that respect  $SO(10)$  is more of an umbrella term, incorporating these different models with alternate symmetry-breaking routes, scalar structures, and physics consequences. What is important for this work is that  $SO(10)$  has the Pati-Salam symmetry ( $\mathcal{G}_{PS}$ ) as a subgroup<sup>4</sup> and includes the discrete D-parity [15] which enforces left-right parity,  $g_L = g_R$ . The Left-Right Symmetric group is embedded in  $\mathcal{G}_{PS}$ . Thus, having reviewed the CMS result in terms of the LRS model, both with and without left-right parity, the obvious next step is to look at it through the lenses of the Pati-Salam partial unified and  $SO(10)$  grand unified theories.

In this section we summarize the features of  $SO(10)$  GUTs which are relevant for our subsequent discussions. We consider the **non-supersymmetric** version of this theory.

#### III.1 Symmetry breaking

Symmetry	$SO(10)$	D-Parity	$SU(4)_C$	$SU(2)_R$	$U(1)_R \times U(1)_{B-L}$	$SU(2)_L \times U(1)_Y$
Breaking Scale	$M_U$	$M_D$	$M_C$	$M_R$	$M_0$	$M_Z$

Table 1: *The different scales at which subgroups of  $SO(10)$  get broken.*

The different ways in which  $SO(10)$  GUT can step-wise break to the SM are graphically represented in Fig. 4. The intermediate energy scales of various stages of symmetry breaking will be denoted according to Table 1. Among these,  $M_D \geq M_R \geq M_0 > M_Z$  always. In order to systematically study the different ways in which  $SO(10)$  can descend to the SM, we first classify them into *routes* based on the order of symmetry breaking. We will call the route with  $M_C \geq M_D \geq M_R$ , CDR (Green, Dashed), the one with  $M_D \geq M_C \geq M_R$ , DCR (Red, Solid), and another with  $M_D \geq M_R \geq M_C$ , DRC (Blue, Dotted). Thus there are essentially three routes with a maximum number of four intermediate stages. Among the intermediate stages the first and the last, namely,  $SU(4)_C \times (SU(2)_L \times SU(2)_R)_D$  ( $\equiv \mathcal{G}_{422D}$ ) and  $SU(3)_C \times U(1)_{B-L} \times SU(2)_L \times U(1)_R$  ( $\equiv \mathcal{G}_{3121}$ ), are common to all routes<sup>5</sup>. The other possible intermediate symmetries, in this notation, are  $\mathcal{G}_{422}$ ,  $\mathcal{G}_{421}$ ,  $\mathcal{G}_{3122D}$ , and  $\mathcal{G}_{3122}$  (see Fig. 4). All models of  $SO(10)$  symmetry breaking (symmetry-breaking *chains*) are thus defined by the route it belongs to and the Higgs multiplets that it includes. Figure 4 essentially shows the *maximum-step chains* (chains with maximum number of intermediate symmetries) of each route. Other chains are essentially subcases of these with multiple symmetries breaking at the same scale. This can be achieved if multiple Higgs

<sup>4</sup> $SO(10)$  can break into  $\mathcal{G}_{SM}$  through two distinct routes, one through an intermediate  $SU(5)$  with no left-right symmetry and another through the PS stage. A longer proton decay lifetime  $\tau_p$  than predicted by minimal  $SU(5)$  and the ease of incorporation of seesaw neutrino masses give the second option a slight preference.

<sup>5</sup>Detailed discussion of D-parity and its breaking at a different scale from  $SU(2)_R$  in  $SO(10)$  models appears in [19].

sub-multiplets gain vacuum expectation value ( $vev$ ) at the same scale or if a single sub-multiplet breaks more than one symmetry.

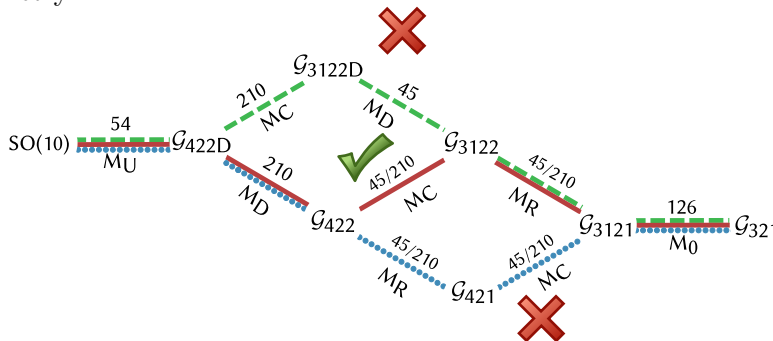


Figure 4: *Symmetry breaking routes of  $SO(10)$  distinguished by the order of breaking of  $SU(2)_R$ ,  $SU(4)_C$ , and  $D$ -parity. The  $SO(10)$  scalar multiplets responsible for symmetry breaking at every stage have been indicated. Only the DCR (red solid) route can accommodate the light  $W_R$  scenario.*

### III.2 Scalar structure and the Extended Survival Hypothesis (ESH)

The gauge bosons in the model and their masses are determined by the symmetry group and its sequential breaking to the SM. The fermions come in three generations in each of which there are the SM quarks and leptons and a right-handed neutrino. Thus it is only the scalar sector which retains a degree of flexibility.

The generation of quark and lepton masses requires a  $\underline{10}$  of  $SO(10)$  while the see-saw mechanism for neutrino masses relies on a  $\underline{126}$ . Their decompositions under the PS group are<sup>6</sup>:

$$10 = [1, 2, 2] + [6, 1, 1] , \quad (2)$$

and

$$126 = [6, 1, 1] + [15, 2, 2] + [10, 3, 1] + [\overline{10}, 1, 3] . \quad (3)$$

These scalars also have important roles in gauge symmetry breakings. The  $vev$  of the  $\underline{10}$ , which is  $\mathcal{O}(M_Z)$ , breaks the standard model  $SU(2)_L \times U(1)_Y$  symmetry while the  $\underline{126}$  is responsible for the breaking of  $U(1)_{B-L} \times U(1)_R$  at the scale  $M_0$ .

In a grand unified theory masses of fermions in the same multiplet are related. In particular, the  $\underline{10}$  of  $SO(10)$  implies  $M_d = M_l^\dagger$ , where  $M_d$  is the mass matrix of  $d$ -type quarks and  $M_l$  that of the charged leptons. Though these relations are valid only at the scale of unification and at lower energies corrections have to be included, even then they are not in consistency with the measured masses. One way to address this issue is to invoke a  $[15, 2, 2]$  submultiplet which is present in the  $\underline{126}$  and the  $\underline{120}$  of  $SO(10)$  to bring the masses closer to their actual values [20, 21]. As we discuss later, a light  $[15, 2, 2]$  scalar submultiplet can help lower the unification scale.

Two other  $SO(10)$  representations which turn out to be useful for symmetry breaking and whose submultiplet structure will be important are the  $\underline{45}$  and  $\underline{210}$ . Under the PS group they consist of:

$$45 = [15, 1, 1] + [6, 2, 2] + [1, 3, 1] + [1, 1, 3] , \quad (4)$$

<sup>6</sup>We will use the notation  $[\phi_4, \phi_L, \phi_R]$  to specify the behaviour of  $SO(10)$  submultiplets under the Pati-Salam symmetry.

$$210 = [1, 1, 1] + [15, 1, 1] + [6, 2, 2] + [15, 3, 1] + [15, 1, 3] + [10, 2, 2] + [\overline{10}, 2, 2] . \quad (5)$$

Even using these limited  $SO(10)$  scalar multiplets<sup>7</sup>, there remains a variety of options for the scalar submultiplets that can be used for the different stages of symmetry breaking indicated in Fig. 4. They affect the unification and intermediate energy scales through their role in the evolution of gauge couplings. We make two restrictions: **(a) Only renormalisable terms** will be kept in the  $SO(10)$ -symmetric lagrangian<sup>8</sup>, and **(b) The Extended Survival Hypothesis, which is a consequence of minimal fine-tuning**, is taken to be valid.

According to ESH [22, 23], at any intermediate energy scale only those scalar submultiplets (under the unbroken symmetry at that stage) which are required to spontaneously break a symmetry at that or any lower energy remain massless. All other submultiplets become massive. Because the normal expectation of scalar masses is to be at the highest energy scale the extended survival hypothesis posits the minimal number of fine-tunings in the scalar sector.

With these guiding principles we now turn to the scalar multiplets that are employed for the descent of  $SO(10)$  to the SM. The first (at  $M_U$ ) and last (at  $M_0$ ) stages of the symmetry breaking in Fig. 4, which are common to all alternate channels, utilise a 54-plet and a 126-plet of scalar fields, respectively. D-parity is broken through the *vev* of D-odd scalars. There is a D-odd PS singlet in the 210 of  $SO(10)$  which can be utilised for this purpose.

### III.3 Renormalisation Group Equations

The one-loop RG evolution for the coupling  $\alpha^g(\mu)$  corresponding to a gauge symmetry  $g$  can be written as:

$$\frac{1}{\alpha^g(\mu_i)} = \frac{1}{\alpha^g(\mu_j)} + \frac{b_{ji}^g}{2\pi} \ln\left(\frac{\mu_j}{\mu_i}\right). \quad (6)$$

$b_{ji}^g$  is the coefficient of the  $\beta$ -function between the scales  $\mu_i$  and  $\mu_j$ :

$$b^g = -\frac{11}{3}N_g + \frac{2}{3}\sum_F T(F_g)d(F_{g'})n_G + \frac{1}{6}\sum_S \delta_S T(S_g)d(S_{g'}), \quad (7)$$

where the three terms are contributions from gauge bosons, chiral fermions, and scalars respectively.  $N_g$  is the quadratic Casimir corresponding to the particular symmetry group  $g$ ,  $N_g$  is 0 for  $U(1)$  and  $N$  for  $SU(N)$ .  $T(F_g)$  and  $d(F_g)$  are the index and the dimension of the representation of the chiral fermion multiplet  $F$  under the group  $g$  and the sum is over all fermion multiplets of one generation.  $n_G$  is the number of fermion generations, 3 in our case. Similarly  $T(S_g)$  and  $d(S_g)$  are the index and the dimension of the representation  $S_g$  of the scalar  $S$  under  $g$ .  $\delta_S$  takes the value 1 or 2 depending on whether the scalar representation is real or complex.

It is worth noting that  $b^g$  is positive for  $U(1)$  subgroups and negative<sup>9</sup> for  $SU(n)$ . Therefore,  $U(1)$  couplings grow with increasing energy while  $SU(n)$  couplings decrease.

<sup>7</sup>A 54 is used for the first step of GUT symmetry breaking. It does not affect the RG running of the couplings.

<sup>8</sup>This excludes, for example, using scalar 16-plets to mimic the  $SO(10)$  126 for neutrino mass through effective dimension-5 terms in the Lagrangian.

<sup>9</sup>Contributions from large scalar multiplets can make the beta-function positive. This does happen for  $SU(2)_R$  in the example we discuss later.



For ease of use, we will rewrite eq. (6) as:

$$w_i^g = w_j^g + \frac{1}{2\pi} b_{ji}^g \Delta_{ji} , \quad (8)$$

where  $w_i^g \equiv \frac{1}{\alpha^g(\mu_i)}$  and  $\Delta_{ji} \equiv \ln\left(\frac{\mu_j}{\mu_i}\right)$ .

If the symmetry  $g$  is broken to  $g'$  at the scale  $\mu_i$  then the coupling constant matching condition is simply  $w_i^g = w_i^{g'}$  unless two groups combine to yield a residual symmetry. As an example of the latter, for  $U(1)_Y$  of the standard model, which results from a linear combination of  $U(1)_R$  and  $U(1)_{B-L}$  at the scale  $M_0$ :

$$w_0^Y = \frac{3}{5}w_0^R + \frac{2}{5}w_0^{B-L} . \quad (9)$$

U(1) mixing not taken into account

Matching all the couplings at the boundaries and imposing the unification condition one arrives at three equations:

$$\begin{aligned} w_Z^3 &= w_U + \frac{1}{2\pi} \sum_i b_{i,i-1}^C \Delta_{i,i-1} , \\ w_Z^{2L} &= w_U + \frac{1}{2\pi} \sum_i b_{i,i-1}^{2L} \Delta_{i,i-1} , \\ w_Z^Y &= w_U + \frac{3}{5} \frac{1}{2\pi} \sum_i b_{i,i-1}^{1R} \Delta_{i,i-1} + \frac{2}{5} \frac{1}{2\pi} \sum_i b_{i,i-1}^{B-L} \Delta_{i,i-1} , \end{aligned} \quad (10)$$

where  $w_U$  is the reciprocal of the coupling strength at unification.  $i$  runs from the unification scale to  $M_0$ .  $C$  stands for  $SU(3)_C$  or  $SU(4)_C$  depending on the energy scale  $\mu$ . Similarly,  $1R$  ( $B-L$ ) in the last equation represents  $U(1)_R$  or  $SU(2)_R$  ( $U(1)_{B-L}$  or  $SU(4)_C$ ).

The left-hand-sides of the three equations in (10) are the inputs fixed by experiments. The equations are linear in  $w_U$  and  $\ln(\mu_i)$  – the logarithms of the mass-scales. There are  $2+m$  variables:  $m$ , the number of scales intermediate to  $M_U$  and  $M_Z$ ,  $w_U$ , the magnitude of the coupling at unification, and the GUT scale  $M_U$  itself. Thus, an  $SO(10)$  chain with one intermediate scale ( $m=1$ ) is a determined system while those with more steps are underdetermined.

## IV Coupling unification and low energy expectations

In the LRS model the energy scales of symmetry breaking can be freely chosen to be consistent with the low energy data. Once embedded in GUTs one must also verify that such choices of intermediate scales are consistent with perturbative unification of the couplings at sub-Planck energies and check their implications for other symmetry-breaking scales. In this section we look at the restrictions imposed by gauge coupling unification together with the CMS result interpreted as a signal of  $W_R$ .

$SO(10)$  can descend to the SM through a maximum of four intermediate stages (Fig. 4). Such four-step symmetry breakings are underdetermined. Accordingly, one is permitted to choose the scale  $M_R$  in the TeV range, as required by the CMS data, and to check the consistency of the equations.  $M_0$  is always below  $M_R$  and thus keeping the latter at a few TeV sets the former to an even lower value.

## IV.1 Pati-Salam partial unification

The PS symmetry with D-parity,  $\mathcal{G}_{422D}$ , is a common intermediate stage for all the  $SO(10)$  symmetry-breaking options. When D-parity is intact, this model has two-independent couplings, namely,  $g_{4C}$  and  $g_{2L} = g_{2R} = g_2$ , which achieve equality at the grand unification scale  $M_U$ . In the DCR and DRC routes the Pati-Salam  $\mathcal{G}_{422}$  survives at the next step but D-parity no longer holds. In contrast, for the CDR route the PS symmetry is broken before D-parity. Needless to say, so long as D-parity remains unbroken  $\eta = 1$ .

In Pati-Salam partial unification one has a set of three equations similar to eq. (10) sans the constraint of grand unification. In place of an inverse GUT coupling  $w_U$  one gets two separate couplings –  $w_C^4$  ( $= w_C^{B-L} = w_C^3$ ) at  $M_C$  and  $w_D^2$  ( $= w_D^{2R} = w_D^{2L}$ ) at  $M_D$ . Thus, the two variables – the GUT coupling and the GUT scale – are replaced by the  $SU(4)_C$  unification coupling and a D-parity symmetric  $SU(2)$  coupling. In the following sections we will look at the results that arise from RG evolution for both PS partial unification and  $SO(10)$  grand unification.

## IV.2 Left-right symmetry and unification

The scalar field contributions to gauge coupling evolution play a significant role in achieving coupling unification while keeping a low  $M_R$ . This has led to a plethora of models where scalar fields have been incorporated in the theory solely for this purpose. This is not the path that we choose. Indeed, the scalar fields which we *do* include become indispensable in some cases. For example, a subcase which one might imagine from Fig. 4 will have  $M_R = M_0$ . The one-step symmetry breaking of  $\mathcal{G}_{3122} \rightarrow \mathcal{G}_{321}$  can be realized through the *vev* of just a  $[\overline{10}, 1, 3] \subset \underline{126}$ , dispensing off the submultiplet which breaks  $SU(2)_R \rightarrow U(1)_R$ . However, without this latter contribution the coupling constants no longer unify. So,  $M_R = M_0 \sim \mathcal{O}(\text{TeV})$  cannot be accommodated without at least the scalar multiplets that we keep.

As mentioned earlier, the three key ingredients in interpreting the CMS result are the ratio between the left- and right-handed gauge couplings,  $\eta$ , the Majorana mass of the right-handed electron neutrino,  $M_{N_e}$ , and the right-handed leptonic mixing  $V_{N_l}$ . The Majorana mass of the right-handed neutrino of the  $l$ -th flavour, in the TeV range, is obtained through the Yukawa coupling  $Y_{126}^l$ . The mass is proportional to the  $\Delta L = 2$  *vev*,  $v_{126}$ , of the  $(1, -2, 1, 1) \subset [\overline{10}, 1, 3] \subset \underline{126}$ . The latter also breaks the  $\mathcal{G}_{3121}$  symmetry. Hence, one has  $M_{N_l} \sim (Y_{126}^l/g_{B-L})M_0$ . The Yukawa coupling,  $Y_{126}^l$ , can be chosen to obtain a desired value of  $M_{N_l}$  without affecting other physics. Thus the choice of  $r = M_N/M_{W_R}$  is decoupled from the analysis of coupling unification.

The mixing in the right-handed lepton sector –  $V_{N_l}$  – is the second relevant quantity in this analysis. It is determined by the generation structure of the Yukawa matrix. Since this does not affect the evolution of couplings, which is the focus, our analysis does not impose any restriction on the choice of this mixing.

The relative strength of the right-handed coupling *vis-à-vis* the left-handed one at the  $SU(2)_R$ -breaking scale –  $\eta = \frac{g_R}{g_L}$  – is, however, intimately related to the RG running of the gauge couplings.

$$w_R^{2R} = \frac{1}{\eta^2} w_R^{2L} . \quad (11)$$

The magnitude of  $\eta$  will vary for symmetry-breaking chains depending on the scalar content of the theory and the energy scales at which different symmetries break. Nonetheless, the minimum value

that can be attained by  $\eta$  is almost independent of the way in which  $SO(10)$  or  $\mathcal{G}_{PS}$  descends to the standard model, as we now discuss. Firstly the requirement that  $M_R$  is  $\mathcal{O}(\text{TeV})$  and  $M_0$  even lower, keeps them close to each other and the two are not too far from  $M_Z$  either. The other feature, noted earlier, is that  $U(1)$  couplings increase as the energy scale  $\mu$  increases while  $SU(n)$  couplings do the opposite.

One starts from eq. (9) which relates the  $U(1)$  couplings when the symmetry breaking  $\mathcal{G}_{3121} \rightarrow \mathcal{G}_{321}$  occurs at  $M_0$ . Obviously,

$$w_0^{1R} > w_R^{1R} = w_R^{2R} = \left(\frac{1}{\eta^2}\right) w_R^{2L} \quad , \quad (12)$$

and from  $w_C^{B-L} = w_C^{3C}$

$$w_0^{B-L} > w_R^{B-L} > w_R^{3C} \quad . \quad (13)$$

From eq. (9) together with eqs. (12) and (13) one has

$$\eta^2 > \frac{3w_R^{2L}}{5w_0^Y - 2w_R^{3C}} \simeq \frac{3w_0^{2L}}{5w_0^Y - 2w_0^{3C}} \quad . \quad (14)$$

The inequality in the first step in eq. (12) is due to the evolution of  $w^{1R}$  from  $M_0$  to  $M_R$ . Since these two energy scales are both in the TeV range this effect is not large. A similar reasoning is also valid for the first inequality in eq. (13) but the second could be much more substantial. Using the current values of the low energy couplings<sup>10</sup> and extrapolating them to  $\mu = M_0$  one gets

$$\eta_{min} \sim 0.59 \quad . \quad (15)$$

We stress that eq. (15) is an artefact of the LRS model so long as there is a merging of the  $U(1)_{B-L}$  with  $SU(3)_C$ , and so is valid for both PS (partial) and  $SO(10)$  (grand) unification. However, this is a limit in principle, accomplishing it will depend on the details of symmetry breaking and the scalar content of the theory. We have previously seen that that the CMS result is compatible with the LRS model for  $S$  as low as  $\sim 0.25$ . From the preceding discussion we see that  $S$  lower than  $\sim 0.59$  cannot be attained by  $\eta$  alone.

## V The three routes of $SO(10)$ symmetry breaking

In this section we consider one by one the three routes depicted in Fig. 4 by which  $SO(10)$  can descend to the SM. We focus on the scalar fields that are required and the intermediate energy scales involved. We use one-loop renormalisation group equations here but have checked that including two-loop effects does not change the results drastically. Since the equations are usually underdetermined, motivated by the CMS data, we will keep  $4 \text{ TeV} \leq M_R \leq 10 \text{ TeV}$  and  $1 \text{ TeV} \leq M_0 \leq 4 \text{ TeV}$  for the chains of descent.

### V.1 The DRC route

Restricting  $M_R$  to the TeV range automatically eliminates the DRC route (Blue dotted in Fig. 4) –  $SU(4)_C$  breaking *after*  $M_R$  – because then the leptoquark gauge bosons of  $SU(4)_C$  achieve a mass of

<sup>10</sup>We use  $\alpha_3 = 0.1185(6)$ ,  $\sin^2 \theta_W = 0.23126(5)$ , and  $\alpha = 1/127.916$  at  $\mu = M_Z$  [24].

the TeV order. Light leptoquarks below  $10^6$  GeV are forbidden from rare decays of strange mesons, such as  $K_L \rightarrow \mu e$  [3, 25, 26]. The DRC route of symmetry breaking is thus not compatible with the CMS result.

## V.2 The CDR route ✗

$SO(10)$ repn.	Symmetry breaking	Scalars contributing to RG				
		$M_Z \leftrightarrow M_0$ $\mathcal{G}_{321}$	$M_0 \leftrightarrow M_R$ $\mathcal{G}_{3121}$	$M_R \leftrightarrow M_D$ $\mathcal{G}_{3122}$	$M_D \leftrightarrow M_C$ $\mathcal{G}_{3122D}$	$M_C \leftrightarrow M_U$ $\mathcal{G}_{422D}$
<b>10</b>	$\mathcal{G}_{321} \rightarrow EM$	(1,2, $\pm 1$ )	(1,0,2, $\pm \frac{1}{2}$ )	(1,0,2,2)	(1,0,2,2) <sub>+</sub>	[1,2,2] <sub>+</sub>
<b>126</b>	$\mathcal{G}_{3121} \rightarrow \mathcal{G}_{321}$	-	(1,-2,1,1)	(1,-2,1,3)	(1,-2,1,3) <sub>+</sub>	$[\overline{10},1,3]$ <sub>+</sub>
		-	-	-	(1,2,3,1) <sub>+</sub>	[10,3,1] <sub>+</sub>
<b>210</b>	$\mathcal{G}_{3122} \rightarrow \mathcal{G}_{3121}$	-	-	(1,0,1,3)	(1,0,1,3) <sub>+</sub>	[15,1,3] <sub>+</sub>
		-	-	-	(1,0,3,1) <sub>+</sub>	[15,3,1] <sub>+</sub>
<b>210</b>	$\mathcal{G}_{3122D} \rightarrow \mathcal{G}_{3122}$	-	-	-	(1,0,1,1) <sub>-</sub>	[1,1,1] <sub>-</sub>
<b>210</b>	$\mathcal{G}_{422D} \rightarrow \mathcal{G}_{3122D}$	-	-	-	-	[15,1,1] <sub>+</sub>

Table 2: Scalar fields considered when the ordering of symmetry-breaking scales is  $M_C \geq M_D \geq M_R$ . The submultiplets contributing to the RG evolution at different stages according to the ESH are shown.  $D$ -parity ( $\pm$ ) is indicated as a subscript.

With all intermediate stages distinct, for this route (Green dashed in Fig. 4) one has:

$$SO(10) \xrightarrow[54]{M_U} \mathcal{G}_{422D} \xrightarrow[210]{M_C} \mathcal{G}_{3122D} \xrightarrow[210]{M_D} \mathcal{G}_{3122} \xrightarrow[210]{M_R} \mathcal{G}_{3121} \xrightarrow[126]{M_0} \mathcal{G}_{321} . \quad (16)$$

The scalar submultiplets responsible for the symmetry breaking are shown in Table 2. An alternative to the above would be to break  $\mathcal{G}_{3122} \rightarrow \mathcal{G}_{3121}$  using a  $[1,1,3] \subset \underline{45}$  in place of the  $[15,1,3] \subset \underline{210}$ . We also comment about this option.

In order to proceed with an elaboration of the consequences associated with this route it is helpful to list the one-loop beta-function coefficients for the stages  $M_R \leftrightarrow M_D$  and  $M_D \leftrightarrow M_C$ . Including the contributions from the scalars in Table 2, fermions, and gauge bosons one finds from eq. (6)

$$\begin{aligned} b_{DR}^3 &= -7, \quad b_{DR}^{B-L} = \frac{11}{2}, \quad b_{DR}^{2L} = -3, \quad b_{DR}^{2R} = -2, \\ b_{CD}^3 &= -7, \quad b_{CD}^{B-L} = 7, \quad b_{CD}^{2L} = -2, \quad b_{CD}^{2R} = -2. \end{aligned} \quad (17)$$

The  $SU(2)_L$  and  $SU(2)_R$  couplings evolve from  $M_R$  to become equal at  $M_D$ . This requires ( $\Delta_{AB} = \ln \frac{M_A}{M_B}$ ):

$$w_R^{2L} - w_R^{2R} = \frac{1}{2\pi} \{ (b_{DR}^{2L} - b_{DR}^{2R}) \Delta_{DR} \} . \quad (18)$$

Similarly the  $SU(3)_C$  and  $U(1)_{B-L}$  couplings become equal at  $M_C$ , i.e.,

$$w_R^3 - w_R^{B-L} = \frac{1}{2\pi} \{ (b_{DR}^3 - b_{DR}^{B-L}) \Delta_{DR} + (b_{CD}^3 - b_{CD}^{B-L}) \Delta_{CD} \} . \quad (19)$$

The left-hand-sides of eqs. (18) and (19) are given in terms of the various couplings at  $M_R$ . Since  $M_R \sim \mathcal{O}(\text{TeV})$  and the RG evolution is logarithmic in energy it is not a bad approximation to assume that they do not change significantly from  $M_Z$  to  $M_R$ , i.e.,  $w_R^i \simeq w_O^i \simeq w_Z^i$ . Then recalling eq. (9) which relates  $w_0^Y$  with  $w_0^R$  and  $w_0^{B-L}$  one can obtain:

$$3w_Z^{2L} + 2w_Z^3 - 5w_Z^Y \simeq \frac{1}{2\pi} \{ [3(b_{DR}^{2L} - b_{DR}^{2R}) + 2(b_{DR}^3 - b_{DR}^{B-L})] \Delta_{DR} + 2(b_{CD}^3 - b_{CD}^{B-L}) \Delta_{CD} \}. \quad (20)$$

Using the beta-function coefficients from eq. (17), one can reexpress eq. (20) as:

$$3w_Z^{2L} + 2w_Z^3 - 5w_Z^Y \simeq \frac{1}{2\pi} \{ 28 \Delta_{CR} \}. \quad (21)$$

Notice that  $M_D$  has dropped out. Further, the low energy values of  $\alpha, \alpha_s$  and  $\sin^2 \theta_W$  [24] then **imply  $M_C \sim 10^{18} M_R$ , i.e., way beyond the Planck scale.** The low energy SM parameters are now quite well-measured and offer no escape route from this impasse. Two-loop contributions also do not change the situation drastically. We have checked that if one breaks  $\mathcal{G}_{3122} \rightarrow \mathcal{G}_{3121}$  through a  $[1,1,3] \subset \underline{45}$  rather than the  $[15,1,3] \subset \underline{210}$  (see Table 2), the change is in the evolution of the couplings in the  $M_C \leftrightarrow M_U$  sector which does not affect this conclusion.

The above analysis does not resort to the constraint of grand unification at all. The results hold for PS partial unification as well. So, the CDR route of descent also has to be abandoned for  $M_R \sim \mathcal{O}(\text{TeV})$ .

### V.3 The DCR route

SO(10) repn.	Symmetry breaking	Scalars contributing to RG				
		$M_Z \leftrightarrow M_0$ $\mathcal{G}_{321}$	$M_0 \leftrightarrow M_R$ $\mathcal{G}_{3121}$	$M_R \leftrightarrow M_C$ $\mathcal{G}_{3122}$	$M_C \leftrightarrow M_D$ $\mathcal{G}_{422}$	$M_D \leftrightarrow M_U$ $\mathcal{G}_{422D}$
<b>10</b>	$\mathcal{G}_{321} \rightarrow EM$	(1,2, $\pm 1$ )	(1,0,2, $\pm \frac{1}{2}$ )	(1,0,2,2)	[1,2,2]	[1,2,2] <sub>+</sub>
<b>126</b>	$\mathcal{G}_{3121} \rightarrow \mathcal{G}_{321}$	-	(1,-2,1,1)	(1,-2,1,3)	$[\overline{10},1,3]$	$[\overline{10},1,3]$ <sub>+</sub> [10,3,1] <sub>+</sub>
<b>210</b>	$\mathcal{G}_{3122} \rightarrow \mathcal{G}_{3121}$	-	-	(1,0,1,3)	[15,1,3]	[15,1,3] <sub>+</sub> [15,3,1] <sub>+</sub>
<b>210</b>	$\mathcal{G}_{422} \rightarrow \mathcal{G}_{3122}$	-	-	-	[15,1,1]	[15,1,1] <sub>+</sub>
<b>210</b>	$\mathcal{G}_{422D} \rightarrow \mathcal{G}_{422}$	-	-	-	-	[1,1,1] <sub>-</sub>

Table 3: Scalar fields considered when the ordering of symmetry-breaking scales is  $M_D \geq M_C \geq M_R$ . The submultiplets contributing to the RG evolution at different stages according to the ESH are shown. D-parity ( $\pm$ ) is indicated as a subscript.

After having eliminated the other alternatives, the only remaining route of descent has the mass ordering  $M_D \geq M_C \geq M_R$  (Red solid in Fig. 4). Keeping all possible intermediate stages separate from each other this corresponds to:

$$SO(10) \xrightarrow[54]{M_U} \mathcal{G}_{422D} \xrightarrow[210]{M_D} \mathcal{G}_{422} \xrightarrow[210]{M_C} \mathcal{G}_{3122} \xrightarrow[210]{M_R} \mathcal{G}_{3121} \xrightarrow[126]{M_0} \mathcal{G}_{321} . \quad (22)$$

In the above we have indicated the  $SO(10)$  multiplets which contribute to symmetry breaking at every stage. The scalar submultiplets which contribute to the RG equations as dictated by ESH are shown in Table 3. There is, however, an alternative which relies on a 45 of  $SO(10)$  whose contents under the Pati-Salam group are given in eq. (4).  $SU(2)_R$  can be broken by the  $(1,0,1,3) \subset [1,1,3] \subset \underline{45}$  replacing the  $[15,1,3] \subset \underline{210}$ . In fact, the  $SU(4)_C$  breaking  $[15,1,1]$  is also present in the 45. However, one cannot entirely dispense with the 210 because the  $[1,1,1]_-$  in it has no analog in the 45.

Denoting by  $h_D, h_C, h_R$  the  $SO(10)$  scalar multiplets responsible for the breaking of D-Parity,  $SU(4)_C$ , and  $SU(2)_R$  respectively, we therefore have the following alternatives:  $\{h_D, h_C, h_R\}$  can be  $\{210, 45, 45\}$ ,  $\{210, 45, 210\}$ ,  $\{210, 210, 45\}$  and  $\{210, 210, 210\}$ . Of these, the first employs the lowest dimensional scalar multiplets required to break symmetries at each scale while the last one uses the least number of  $SO(10)$  scalar multiplets. Using 45 or 210 for  $h_C$  makes no difference in the physics since in both cases a  $[15,1,1]$  Pati-Salam submultiplet is used. The distinction is relevant only in the choice of  $h_R$ .

The one-loop beta-function coefficients for the couplings in the  $M_R \leftrightarrow M_C$  and  $M_C \leftrightarrow M_D$  energy ranges obtained using eq. (6) and the scalars in Table 3 are:

$$\begin{aligned} b_{CR}^3 &= -7, \quad b_{CR}^{B-L} = \frac{11}{2}, \quad b_{CR}^{2L} = -3, \quad b_{CR}^{2R} = -2, \\ b_{DC}^4 &= -5, \quad b_{DC}^{2L} = -3, \quad b_{DC}^{2R} = \frac{26}{3}. \end{aligned} \quad (23)$$

The  $SU(4)_C$  and  $U(1)_{B-L}$  couplings evolve to become equal at  $M_C$ . Thus

$$w_R^3 - w_R^{B-L} = \frac{1}{2\pi} \left\{ (b_{CR}^3 - b_{CR}^{B-L}) \Delta_{CR} \right\} . \quad (24)$$

Matching of the  $SU(2)_L$  and  $SU(2)_R$  couplings at  $M_D$  implies:

$$w_R^{2L} - w_R^{2R} = \frac{1}{2\pi} \left\{ (b_{CR}^{2L} - b_{CR}^{2R}) \Delta_{CR} + (b_{DC}^{2L} - b_{DC}^{2R}) \Delta_{DC} \right\} . \quad (25)$$

As before, we use the approximation  $w_R^i \simeq w_O^i \simeq w_Z^i$  and combine eqs. (24) and (25) to get:

$$3w_Z^{2L} + 2w_Z^3 - 5w_Z^Y \simeq \frac{1}{2\pi} \left\{ [3(b_{CR}^{2L} - b_{CR}^{2R}) + 2(b_{CR}^3 - b_{CR}^{B-L})] \Delta_{CR} + 3(b_{DC}^{2L} - b_{DC}^{2R}) \Delta_{DC} \right\} . \quad (26)$$

A special limit of the DCR route is when  $M_D = M_C$ , i.e.,  $\Delta_{DC} = \ln \frac{M_D}{M_C} = 0$ . In this limiting case there is no distinction between this route and the CDR one. Indeed, setting  $M_D = M_C$  in eq. (26) and substituting the beta-function coefficients from eq. (23) one exactly reproduces (21) which places the solution in an unacceptable energy regime.

That one should nonetheless expect acceptable solutions can be surmised from the fact that eq. (26) implies

$$\begin{aligned} \frac{d \ln M_C}{d \ln M_D} &= \frac{3(b_{DC}^{2L} - b_{DC}^{2R})}{[3(b_{DC}^{2L} - b_{DC}^{2R} - b_{CR}^{2L} + b_{CR}^{2R}) - 2(b_{CR}^3 - b_{CR}^{B-L})]} \\ &= 5, \end{aligned} \quad (27)$$

where in the last step we have used eq. (23). This indicates that  $M_C$  changes faster than  $M_D$  and so starting from the  $M_D = M_C$  limit solutions in the DCR route with the symmetry breaking scales below  $M_{Planck}$  are feasible. Replacing the 210 in  $h_R$  by a 45 reduces  $b_{DC}^{2R}$  so much that unification of couplings is no longer possible. In the next section we present the allowed solutions in detail.

## VI $SO(10)$ unification with $M_R \sim \mathcal{O}(\text{TeV})$

In the previous section we have seen that of the three routes of symmetry breaking accessible to  $SO(10)$ , DRC is trivially eliminated when the twin requirements  $M_R \sim \mathcal{O}(\text{TeV})$  and  $M_R > M_C$  are imposed. We also indicated that with the minimal scalar content and following the extended survival hypothesis for the CDR route requiring  $M_R \sim \mathcal{O}(\text{TeV})$  implies that  $M_C > M_{Planck}$ . The only route that can accommodate  $M_R \sim \mathcal{O}(\text{TeV})$  is DCR.

To simplify the discussion, in eq. (26) we have ignored the running of the couplings between  $M_Z$  and  $M_R$ . In obtaining the results presented in this section we have not used such an approximation.

### VI.1 Pati-Salam partial unification for the maximum-step case

The maximum-step symmetry-breaking DCR route has been given in eq. (22). Before turning to  $SO(10)$  we briefly remark about Pati-Salam partial unification within this route. Because there are four steps of symmetry breaking this is an underdetermined system. For this work,  $M_R$  is restricted to be in the  $\mathcal{O}(\text{TeV})$  range. The scale  $M_C$  is taken as the other input in the analysis. At the one-loop level the results can be analytically calculated using the beta-function coefficients in eq. (23). The steps can be identified from eqs. (25) and (26). The latter determines  $M_D$  once  $M_C$  is chosen.  $\eta$  is then fixed using eq. (25).

For example, for  $M_C = 10^6$  GeV one gets  $\eta = 0.63$  when  $M_R = 5$  TeV. Within the Pati-Salam model the upper limit of  $M_D$  is set by the Planck mass  $M_{Planck}$ . We find that in such a limit one has  $M_C = 10^{17.6}$  GeV and  $\eta = 0.87$  for  $M_R = 5$  TeV.

### VI.2 Coupling unification for the maximum-step case

For  $SO(10)$  grand unification one must find the energy scale at which the common  $SU(2)_{L,R}$  coupling beyond  $M_D$  equals the  $SU(4)_C$  coupling, i.e.,  $g_2 = g_{4C}$ . This now sets the upper limit of  $M_C$ .

In the left panel of Fig. 5 we plot  $\eta$  as a function of  $M_C$ . In the inset is shown the behaviour of  $M_U$  and  $M_D$  as functions of  $M_C$ . Due to the unification constraint, the upper limits of  $M_C$ ,  $M_D$  and  $\eta$  all decrease from the respective values which were obtained in the PS case. The lowest value of  $\eta$  turns out to be  $\sim 0.63$ . Notice that a lower value of  $M_C$  is associated with a higher  $M_U$ , which must not exceed  $M_{Planck}$ .  $M_C$  is also bounded from below by the experimental limits on flavour-changing transitions such as  $K_L \rightarrow \mu e$ . It is the latter that determines the lowest admissible  $M_C$ , in general. From the inset it is seen that although  $M_U$  increases as  $M_C$  decreases, it remains below  $M_{Planck}$  so long as  $M_C > 10^6$  GeV. As  $M_C$  increases  $M_D$  increases as well and the point where it meets the decreasing  $M_U$  determines the upper limit of  $M_C$ . For every plot the ranges consistent with  $4 \text{ TeV} \leq M_R \leq 10 \text{ TeV}$  are between the two curves, the solid one indicating the  $M_R = 4$  TeV end. The results are almost insensitive to the choice of  $M_0$  between 1 TeV and  $M_R$ . Note that irrespective of the scale of  $SU(4)_C$  breaking,  $M_D$  always remains above  $10^{16}$  GeV. The unification coupling constant,  $w_U$ , varies between 38.4 and 47.6 so that perturbativity remains valid throughout.

The behaviour of the coupling constants as a function of the energy scale for a typical case of  $M_0 = 1$  TeV,  $M_R = 5$  TeV and  $M_C = 10^{10}$  GeV are shown (solid lines) in the right panel of Fig. 5. Note that due to the contributions of large scalar multiplets to the  $\beta$ -functions the coupling  $g_{2R}$  grows beyond

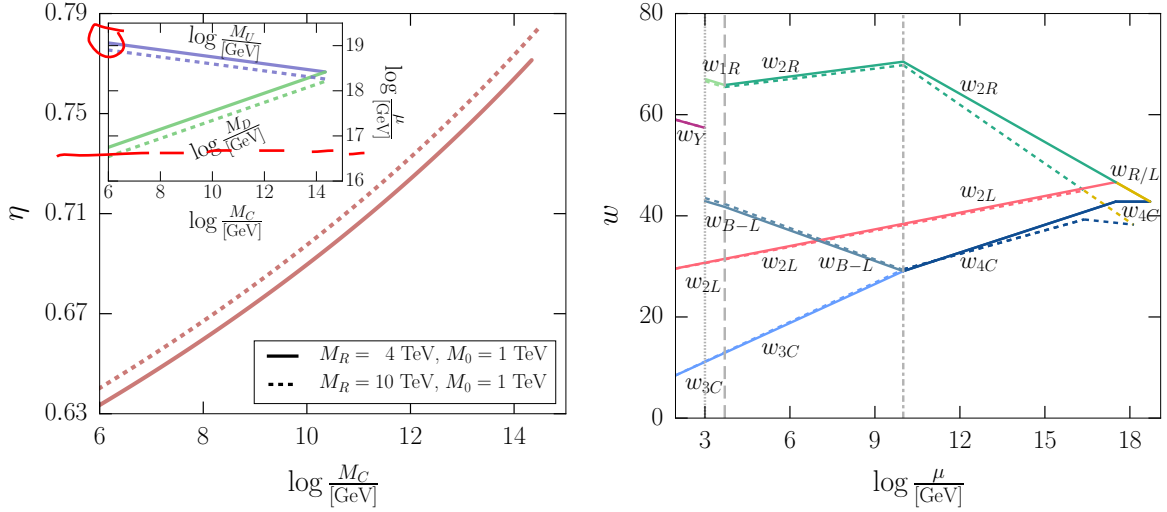


Figure 5: *Left:*  $\eta$  is plotted as a function of  $M_C$  for the DCR route. In the inset the behaviour of  $M_D$  and  $M_U$  are shown. The two curves in each case correspond to  $M_R = 4$  (solid) and 10 TeV (dashed). In both cases  $M_0 = 1$  TeV is taken. *Right:* Behaviour of the gauge couplings for the DCR chain of  $SO(10)$  GUT with  $M_0 = 1$  TeV,  $M_R = 5$  TeV and  $M_C = 10^{10}$  GeV. The solid (dashed) lines correspond to one-loop (two-loop) evolution of couplings. The scalar fields are as in Table 3.

$M_C$ . Although this chain is suited to our needs, the unification scale is close to the Planck scale for  $M_R \sim \mathcal{O}(\text{TeV})$ . Thus, if  $M_{W_R} \sim \mathcal{O}(\text{TeV})$  then it is unlikely that ongoing proton decay experiments [27] will observe a signal. This is a consequence of our adhering to the principle of minimality of Higgs scalars. One can lower  $M_U$  by including scalars redundant to symmetry breaking.

We have set the lower limit of  $M_C$  at  $10^6$  GeV from the limits on rare meson decays such as  $K_L \rightarrow \mu e$  or  $B_{d,s} \rightarrow \mu e$ . The current limit on the branching ratio for the former process is  $Br(K_L \rightarrow \mu^\pm e^\mp) < 4.7 \times 10^{-12}$  at 90% CL [24] which translates to  $M_C \gtrsim 10^6$  GeV. LHCb has set the tightest bounds on the latter processes. They find (again at 90% CL) [28]  $Br(B_d^0 \rightarrow \mu^\pm e^\mp) < 2.8 \times 10^{-9}$  and  $Br(B_s^0 \rightarrow \mu^\pm e^\mp) < 1.1 \times 10^{-8}$  which yield a weaker limit on  $M_C$ . It can be expected that these bounds will be strengthened when the results from the newer runs of LHC appear. In addition,  $n - \bar{n}$  oscillations can be mediated through coloured scalars belonging to the  $[\overline{10}, 1, 3] \subset \underline{126}$  which also acquire mass at the scale of  $M_C$ . The current experimental limit,  $\tau_{n-\bar{n}} \geq 2.7 \times 10^8 \text{s}$  [29] at 90% CL, also translates to  $M_C \gtrsim 10^6$  GeV. Therefore improvements in the measurement of the above-noted rare meson decays and  $n - \bar{n}$  oscillations open the possibility of probing, at least in part, the GUT options that can accommodate a TeV-scale  $W_R$ .

### VI.3 The $M_D = M_U$ case

There are a number of daughter chains of the DCR route with two symmetries breaking at the same scale. Of these, the choice  $M_C = M_R$ , resulting in a common point of the DCR and DRC routes, violates the lower bound on  $M_C$  from flavour changing processes since  $M_R \sim \mathcal{O}(\text{TeV})$ . As noted in the previous section, another alternative, namely,  $M_D = M_C$ , which is a point shared by the DCR and CDR routes, occurs at an energy beyond the Planck scale. The only remaining possibility is  $M_D = M_U$ .

The upper limit on  $M_C$  is set by the requirement  $M_D = M_U$ . This happens when D-parity is broken



at the GUT scale by a  $[1,1,1]_- \subset \underline{210}$ . We thus have

$$SO(10) \xrightarrow[\underline{210}]{M_U=M_D} \mathcal{G}_{422} \xrightarrow[\underline{210}]{M_C} \mathcal{G}_{3122} \xrightarrow[\underline{210}]{M_R} \mathcal{G}_{3121} \xrightarrow[\underline{126}]{M_0} \mathcal{G}_{321} \quad . \quad (28)$$

From the inset in the left panel of Fig. 5 it is seen that for  $M_C \sim 2 \times 10^{14}$  GeV one has  $M_D = M_U$ . As this chain has three intermediate steps, there are no free parameters after setting  $M_0$  and  $M_R$ . The coupling at unification,  $w_U$ , comes to be around 47.6, and  $\eta$ , as can be seen from the left panel of Fig. 5, is near 0.78. An interesting aspect of this chain is that it is minimal in the number of scalar multiplets used.

#### VI.4 Two-loop comparison

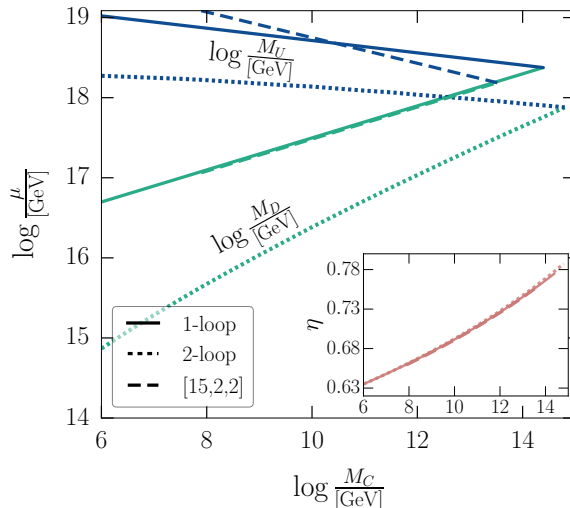


Figure 6: A comparison of the results for one-loop (solid lines) and two-loop (dotted line) running. The evolution of  $M_U$  and  $M_D$  with  $M_C$  is displayed. Also shown is the case of one-loop running when a  $[15,2,2]$  scalar multiplet is added (dashed lines). In the inset the variation of  $\eta$  is presented.

The discussion till now, based on RG evolution using one-loop  $\beta$ -functions, was amenable to an analytical examination. Our aim was to reason our way through different  $SO(10)$  symmetry-breaking options in search of chains which can accommodate a TeV range  $M_R$ . Now, after finding a specific pattern for which  $M_R \sim \mathcal{O}(\text{TeV})$  is tenable, we indicate the size of the two-loop effects for this chain. In the right panel of Fig. 5 the evolution of the couplings for a typical choice of  $M_C = 10^{10}$  GeV,  $M_R = 5$  TeV and  $M_0 = 1$  TeV are indicated by the dashed lines. **It is seen that the essential physics is largely unaltered though there is some change in the various energy scales.**

The chain in (22) contains many scalar fields until  $SU(4)_C$  breaking, contributing heavily to the two-loop  $\beta$ -coefficients [30, 31]. These are responsible for some departures from the one-loop results. We have presented the one-loop results for the DCR route keeping  $M_C$  as an input parameter. In Fig. 6 we compare the one-loop (solid lines) and two-loop (dotted lines) results for  $M_U$  and  $M_D$  as a function of  $M_C$ . The deviation for both scales increases with decreasing  $M_C$ . This is intuitive because with lower  $M_C$   $SU(4)_C$  remains a good symmetry for a larger energy range over which the two-loop contributions are effective. In the inset a similar comparison is made for  $\eta$ . **It is noteworthy that  $\eta$  remains essentially unaffected.**

## VI.5 Additional scalars: an example

If fermion masses are generated through scalars which belong to the minimal set required for symmetry breaking then mass relationships do not reflect observed values. One needs to add at least one extra scalar multiplet – which is light, couples to fermions, and develops a  $vev$  at the electroweak scale – to get realistic mass ratios. In  $SO(10)$ , fermions reside in the  $\underline{16}$  representation and scalars transforming only as  $\underline{120}$ ,  $\underline{126}$ , and  $\underline{10}$  can have Yukawa coupling to fermions, since:

$$16 \times 16 = 10 + 120 + 126 \quad . \quad (29)$$

In  $SO(10)$  GUTs improved fermion mass relations can be obtained [21] using the PS submultiplet  $[15,2,2] \subset \underline{126}$  in addition to the  $[1,2,2] \subset \underline{10}$ . The natural scale for the extra scalar submultiplet would have been at the GUT scale and extra fine-tuning is necessary to keep it at the electroweak scale.

We have examined the behaviour of gauge coupling evolutions for the DCR case including the additional  $[15,2,2]$  submultiplet to check if the TeV range  $M_R$  still remains viable. In Fig. 6 the variation of  $M_D$  and  $M_U$  with  $M_C$  when an extra  $[15,2,2]$  is included are shown (dashed lines). The effect on  $\eta$  (shown in the inset) is negligible. The important change is that the permitted lowest  $M_C$  is more restricted as  $M_U$  tends rapidly towards  $M_{Planck}$ .

It is clear that the scale  $M_D$  is governed by the difference in the  $\beta$ -coefficients of  $SU(2)_R$  and  $SU(2)_L$ . Submultiplets such as  $[15,2,2]$ , which contribute symmetrically to the  $\beta$ -coefficients of the left- and right-handed  $SU(2)$  groups, will not affect the difference and so do not change the D-parity breaking scale. For the reasoning  $\eta$  is not affected as well.

## VII Summary and Conclusions

The observation by the CMS collaboration of a  $2.8\sigma$  excess in the  $(2e)(2j)$  channel around 2.1 TeV can be interpreted as a preliminary indication of the production of a right-handed gauge boson  $W_R$ . Within the left-right symmetric model the excess identifies specific values of  $\eta = g_R/g_L$ ,  $r = M_{N_e}/M_{W_R}$ , and  $V_{N_e e}$ . We stress that even with  $g_R = g_L$  and  $V_{N_e e} = 1$  the data can be accommodated by an appropriate choice of  $r$ .

We explore what the CMS result implies if the left-right symmetric model is embedded in an  $SO(10)$  GUT.  $\eta \neq 1$  is a consequence of the breaking of left-right D-parity. We find that a  $W_R$  in the few TeV range very tightly restricts the possible routes of descent of the GUT to the standard model. The only sequence of symmetry breaking which is permitted is  $M_D > M_C > M_R$  with a D-parity breaking scale  $\geq 10^{16}$  GeV. All other orderings of symmetry breaking are excluded. Breaking of left-right discrete parity at such a high scale pushes  $g_L$  and  $g_R$  apart and one finds  $0.64 \leq \eta \leq 0.78$ . The unification scale,  $M_U$ , has to be as high as  $\sim 10^{18}$  GeV so that it is very unlikely that proton decay will be seen in the ongoing experiments. The  $SU(4)_C$ -breaking scale,  $M_C$ , can be as low as  $10^6$  GeV, which may be probed by rare decays such as  $K_L \rightarrow \mu e$  and  $B_{d,s} \rightarrow \mu e$  or  $n - \bar{n}$  oscillations. In Table [4] we summarise the essence of the allowed GUT solutions. We have assumed that no extra scalar multiplets are included beyond those needed for symmetry breaking and invoked the Extended Survival Hypothesis to identify scalar submultiplet masses.

The ATLAS collaboration has also presented evidence [32] for an enhancement around 2 TeV in the di-boson –  $ZZ$  and  $WZ$  – channels in their 8 TeV data. Our interpretation of the excess in the  $(ee)(jj)$

Sr No.	Intermediate Symmetries	Mass Scales $\left(\log \frac{\mu}{[\text{GeV}]}\right)$			$w_U$	$\eta$
		$M_U$	$M_D$	$M_C$		
1	$\mathcal{G}_{422D} \rightarrow \mathcal{G}_{422} \rightarrow \mathcal{G}_{3122} \rightarrow \mathcal{G}_{3121}$	19.02 - 18.38	16.70 - 18.38	6.00 - 14.39	38.41 - 47.63	0.64 - 0.78
2	2-loop	18.27 - 17.88	14.87 - 17.88	6.00 - 14.80	29.54 - 46.66	0.64 - 0.79
3	Added [15,2,2] scalar	$M_{Planck}$ - 18.19	17.06 - 18.19	7.90 - 13.52	18.59 - 37.52	0.66 - 0.76

Table 4: *The  $SO(10)$  symmetry-breaking chains consistent with  $M_R = 5$  TeV and  $M_0 = 1$  TeV. The intermediate symmetries and the associated mass-scales are shown.*

channel in terms of a  $W_R$  by itself fails to provide an explanation of the above. If the  $W_R$  production is normalised to the former then it falls an order of magnitude short of the di-boson rates. **It has been shown that interpretation of the di-boson observations as well as the  $(ee)(jj)$  data is possible if the LRS model is embellished with the addition of some other fermionic states [33, 34].**

**Acknowledgements:** TB acknowledges a Junior Research Fellowship from UGC, India. AR is partially funded by the Department of Science and Technology Grant No. SR/S2/JCB-14/2009.

## References

- [1] R. N. Mohapatra and J. C. Pati, Phys. Rev. D **11**, 566 (1975); *ibid.* D **11**, 2558 (1975).
- [2] G. Senjanovic and R. N. Mohapatra, Phys. Rev. D **12**, 1502 (1975).
- [3] J. C. Pati and A. Salam, Phys. Rev. D **8**, 1240 (1973).
- [4] H. Georgi, AIP Conf. Proc. **23**, 575 (1975).
- [5] H. Fritzsch and P. Minkowski, Annals Phys. **93**, 193 (1975).
- [6] V. Khachatryan *et al.* [CMS Collaboration], Eur. Phys. J. C **74**, 3149 (2014) [arXiv:1407.3683 [hep-ex]].
- [7] S. Chatrchyan *et al.* [CMS Collaboration], Phys. Rev. Lett. **109**, 261802 (2012) [arXiv:1210.2402 [hep-ex]]; S. Chatrchyan *et al.* [CMS Collaboration], JHEP **1405**, 108 (2014) [arXiv:1402.2176 [hep-ex]].
- [8] G. Aad *et al.* [ATLAS Collaboration], Eur. Phys. J. C **72**, 2056 (2012) [arXiv:1203.5420 [hep-ex]]; G. Aad *et al.* [ATLAS Collaboration], Phys. Rev. Lett. **109**, 081801 (2012) [arXiv:1205.1016 [hep-ex]].
- [9] F. F. Deppisch, T. E. Gonzalo, S. Patra, N. Sahu and U. Sarkar, Phys. Rev. D **90**, 053014 (2014) [arXiv:1407.5384 [hep-ph]]; *ibid.* D **91**, 015018 (2015) [arXiv:1410.6427 [hep-ph]].
- [10] M. Heikinheimo, M. Raidal and C. Spethmann, Eur. Phys. J. C **74**, 3107 (2014) [arXiv:1407.6908 [hep-ph]].

- [11] J. A. Aguilar-Saavedra and F. R. Joaquim, Phys. Rev. D **90** 115010 (2014) [arXiv:1408.2456 [hep-ph]].
- [12] J. Gluza and T. Jeliaski, Phys. Lett. B **748**, 125 (2015) [arXiv:1504.05568 [hep-ph]].
- [13] B. A. Dobrescu and A. Martin, Phys. Rev. D **91**, 035019 (2015) [arXiv:1408.1082 [hep-ph]].
- [14] M. K. Parida and B. Sahoo, arXiv:1411.6748 [hep-ph].
- [15] D. Chang, R. N. Mohapatra and M. K. Parida, Phys. Rev. Lett. **52**, 1072 (1984); Phys. Rev. D **30**, 1052 (1984).
- [16] T. W. B. Kibble, G. Lazarides and Q. Shafi, Phys. Rev. D **26**, 435 (1982).
- [17] V. A. Kuzmin and M. E. Shaposhnikov, Phys. Lett. B **92**, 115 (1980).
- [18] W. Y. Keung and G. Senjanovic, Phys. Rev. Lett. **50**, 1427 (1983).
- [19] D. Chang, R. N. Mohapatra, J. Gipson, R. E. Marshak and M. K. Parida, Phys. Rev. D **31**, 1718 (1985).
- [20] H. Georgi and C. Jarlskog, Phys. Lett. B **86**, 297 (1979).
- [21] H. Georgi and D. V. Nanopoulos, Nucl. Phys. B **159**, 16 (1979).
- [22] F. del Aguila and L. E. Ibanez, Nucl. Phys. B **177**, 60 (1981).
- [23] R. N. Mohapatra and G. Senjanovic, Phys. Rev. D **27**, 1601 (1983).
- [24] K. A. Olive *et al.* [Particle Data Group Collaboration], Chin. Phys. C **38**, 090001 (2014).
- [25] N. G. Deshpande and R. J. Johnson, Phys. Rev. D **27**, 1193 (1983).
- [26] M. K. Parida and B. Purkayastha, Phys. Rev. D **53**, 1706 (1996).
- [27] K. Abe *et al.* [Super-Kamiokande Collaboration], Phys. Rev. Lett. **113**, 121802 (2014) [arXiv:1305.4391 [hep-ex]].
- [28] R. Aaij *et al.* [LHCb Collaboration], Phys. Rev. Lett. **111**, 141801 (2013) [arXiv:1307.4889 [hep-ex]].
- [29] K. Abe *et al.* [Super-Kamiokande Collaboration], Phys. Rev. D **91**, 072006 (2015) [arXiv:1109.4227 [hep-ex]].
- [30] D. R. T. Jones, Phys. Rev. D **25**, 581 (1982).
- [31] M. E. Machacek and M. T. Vaughn, Nucl. Phys. B **222**, 83 (1983); *ibid.* B **236**, 221 (1984); *ibid.* B **249**, 70 (1985).
- [32] G. Aad *et al.* [ATLAS Collaboration], arXiv:1506.00962 [hep-ex].
- [33] P. S. B. Dev and R. N. Mohapatra, arXiv:1508.02277 [hep-ph];
- [34] B. A. Dobrescu and Z. Liu, arXiv:1506.06736 [hep-ph].